Calibration of Free-Flow Radial Gates with Refined Energy Relations

A.J. Clemmens[1], Member, ASCE, and T.L. Wahl, Member[2], ASCE

Abstract: Laboratory experiments were conducted on a radial gate to evaluate the energy equation for free-flow calibration. The experiments were used to develop new equations for the radial gate contraction coefficient for free flow. These were compared to equations for the contraction coefficient of radial and vertical sluice gates developed from prior studies and potential flow theory. The new radial gate free-flow contraction coefficient was related to both the gate lip angle and the gate opening relative to energy head on the gate. The pressure distribution and velocity distribution coefficients were also evaluated. The energy loss through the gate was expressed as a function of the velocity head in the vena contracta, with a gate energy loss coefficient that varies with the relative gate opening. With the revised energy equations, the free-flow discharge predictions were computed for three data sets: 1) the data presented here (USWCL), 2) data from Tel (2000), and 3) data from Buyalski (1983). The coefficients were developed based on the USWCL data only. The average discharge computation error for the combined data sets was 0.37%, and the standard deviation was 1.03%. Submerged flow predictions are the subject of future work.

Introduction

Several methods have been developed for the calibration of sluice and radial gates under free-flow conditions. Henderson (1966) outlined a basic energy-momentum procedure for sluice gates. For radial gates, Clemmens et al. (2003) developed a calibration procedure for both free and submerged flow that used the energy equation on the upstream side of the gate and the momentum equation on the downstream side, the E-M method. This method included empirical factors to account for upstream energy loss, velocity-distribution effects, downstream channel wall forces, and submerged hydraulic jumps. The method can be used to calibrate gates with any upstream and downstream channel size and shape, and thus has advantages over the strictly energy-based methods. This paper evaluates use of just the energy equation under free-flow conditions.

Montes (1997) evaluated the contraction coefficient for planar free-flow sluice gates based on potential flow theory and showed that it varied with gate angle and relative gate opening. Belaud et al. (2009) used momentum balances, with the pressure force exerted on the gate given by potential flow theory, to develop contraction coefficients for sluice gates in both free and submerged flow. Their results generally followed the relationships developed by Montes (1997) and Cassan and Belaud (2012).

Following initial development of the E-M method for radial gates, additional experimental data were collected during 2004 and 2005 in the hydraulics laboratory of

[1] Retired, Laboratory Director, U.S. Arid Land Agricultural Research Center, Maricopa, AZ 85138, albert.clemmens@outlook.com ORCID 0000-0002-8571-068X
[2] Hydraulic Engineer, U.S. Bureau of Reclamation, Hydraulic Investigations and Laboratory Services Group, Denver, CO twahl@usbr.gov

the U.S. Water Conservation Laboratory before it was closed in 2006. The purpose of these experiments was to refine the method presented in Clemmens et al. (2003), particularly the various coefficients used to determine discharge. (Clemmens and Wahl 2012). The analysis by Clemmens et al. (2003) used data reported by Tel (2000).

In this paper, results are presented from analysis of the new experimental data and two previously collected data sets. New radial gate contraction coefficient equations are developed. The energy equation was also modified to include velocity-distribution and pressure-distribution coefficients that account for deviation from hydrostatic pressures and uniform velocity profiles. This gives the energy equation a stronger theoretical foundation.

Theory

Energy Equation

The Energy-Momentum method suggested by Henderson (1966) and developed by Clemmens, et al. (2003) uses the energy equation upstream from the vena contracta and the momentum equation downstream. The energy equation is redeveloped here, considering non-uniform velocity distributions and non-hydrostatic pressure distributions. The general energy and momentum equations for open channel flow are derived in Henderson (1966) without those refinements. For steady flow, the energy equation between sections 1 and 2 in Figure 1 is:

$$H_1 = \lambda_{E1} y_1 + \alpha_1 \frac{v_1^2}{2g} = \lambda_{E2} y_2 + \alpha_2 \frac{v_2^2}{2g} + \Delta H_{12} \qquad (1)$$

where y is flow depth, v is average flow velocity, g is acceleration due to gravity, α is the velocity-distribution coefficient, ΔH_{12} is the energy loss between sections 1 and 2, and the λ_E coefficients account for the effects of a non-hydrostatic pressure distribution in the energy equation. Ideally, section 2 is located at the free-flow vena contracta position. Relationships for the pressure-distribution coefficient, λ_E, and the velocity-distribution coefficient, α, are discussed below. In Clemmens, et al. (2003), the gate energy loss ΔH_{12} was computed as a function of the velocity at section 2. With this assumption, Eq. (1) can be rearranged to read:

$$\lambda_{E1} y_1 + \alpha_1 \frac{v_1^2}{2g} = \lambda_{E2} y_2 + \alpha_2 \frac{v_2^2}{2g} + \xi_2 \left(\frac{v_2^2}{2g}\right) \qquad (2)$$

where ξ_2 is the gate energy loss coefficient.

For a rectangular gate in free flow, the depth at section 2 is equal to the vena contracta or jet depth, y_j, which is usually computed with an empirically determined gate contraction coefficient, δ,

$$y_2 = y_j = \delta w \qquad (3)$$

where w is the gate opening. In Fig. 1, θ is the angle of the gate lip relative to the horizontal, r is the gate radius, and T is the height of the trunnion pin.
Substituting $Q/(b_2 y_2)$ for v_2 in Eq. (2) and solving for discharge gives:

$$Q = b_2 \delta w \sqrt{\frac{2g(H_1 - \lambda_{E2}\delta w)}{\alpha_2 + \xi_2}} \tag{4}$$

where b_2 is the width of the gate and H_1 is determined from the first part of Eq. (1). Eq. (4) is similar to that developed by Clemmens et al. (2003). The only difference is the addition of the pressure distribution coefficient.

Clemmens et al. (2003) developed relationships for $\alpha_2 + \xi_2$ as a function of Reynolds number, neglecting the pressure distribution coefficient. Wahl (2005) refined this relationship based on data from Buyalski (1983). In those relations, $\alpha_2 + \xi_2$ got smaller for prototype structures, since $\xi_2 \rightarrow 0$ as the Reynolds number gets larger. This relationship will be examined with the new data and new equations.

Velocity Distribution Coefficient

Hydraulic theory suggests that the velocity distribution is uniform with an α coefficient close to 1.0 after a disturbance, and gradually approaches a slightly non-uniform distribution due to channel frictional resistance. A common assumption is that it approaches a power-law distribution, where the velocity at a distance y' from the boundary is related to the fraction of the depth, $Y=y'/y$, raised to a power, typically about 1/6 to 1/7. When the power is 1/6, the velocity distribution coefficient, $\alpha = 1.034$. A power of 1/7 gives $\alpha = 1.03$. For measurement flume design, Clemmens et al. (2001) suggest $\alpha_1 = 1.04$. In laboratory studies, Belaud et al. (2012) found average values of $\alpha_1 = 1.045$ and $\alpha_2 = 1.038$, with considerable scatter. For this analysis, 1.04 is used for both α_1 and α_2.

Gate Contraction Coefficients

Tel (2000) developed an equation for the free flow contraction coefficients of sharp-edged radial gates:

$$\delta(\theta)_F = 1.001 - 0.2349\theta - 0.1843\theta^2 + 0.1133\theta^3 \tag{5}$$

where θ is the gate lip angle in radians. He did not consider any variation with relative gate opening.

Belaud et al. (2009) used the momentum equation with gate forces determined from potential flow theory to determine the contraction coefficient for vertical sluice gates, for which the gate lip angle is constant, $\theta = \pi/2$. The solution varied with the relative gate opening, $a = w/H_1$, and as a function of α. (It appears that the same value of α was used for all sections. Here, we refer to α_2.) Belaud (Gilles Belaud personal communication 2012) provided tabular data for the free-flow contraction coefficient for various values of α_2 resulting from the analysis from Belaud et al. (2009). The contraction coefficient at $a = 0$ and $\alpha_2 = 1$ was 0.618. But at $a = 0$ and $\alpha_2 = 1.04$, the contraction coefficient was 0.649. The contraction coefficients for $\alpha_2 = 1.0$ and for $\alpha_2 = 1.04$ were approximated with the following equations:

$\delta\left(\frac{\pi}{2}, a\right)_F = \delta\left(\frac{\pi}{2}, 0\right)_F - 0.06a + 0.026a^2 + 0.026a^3$	$\alpha_2 = 1.0$	(6a)

$\delta\left(\frac{\pi}{2},a\right)_F = \delta\left(\frac{\pi}{2},0\right)_F - 0.056a + 0.039a^2 + 0.056a^3 + 0.026a^4 + 0.025a^5 - 0.021a^6 - 0.675a^7 + 0.970a^8$	$\alpha_2 = 1.04$	(6b)

where $\delta(\pi/2,0)_F$ is the free flow contraction coefficient for a vertical gate ($\delta = 0.618$ for $\alpha_2 = 1.00$ or $\delta = 0.649$ for $\alpha_1 = 1.04$). The eighth order function was necessary to fit the data provided by Belaud for $\alpha_2 = 1.04$, allowing the relationship to curve more sharply upward at higher values of a. These equations will be discussed in the results section, where the experimental data collected in this study will be used to determine an equation for the free-flow contraction coefficient δ_F as a function of both θ and a, namely $\delta(\theta,a)_F$.

Combined Coefficient

The previous analysis by Clemmens et al. (2003) suggested that their combined velocity distribution and energy loss coefficient, $\alpha_2 + \xi_2$, was related to the Reynolds Number for the flow approaching the gate, Re, where

$$Re = \frac{v_g Rh_1}{\upsilon} \tag{7}$$

where v_g is the velocity through the gate opening ($Q/w/b_2$), Rh_1 is the hydraulic radius of the approaching flow, and υ is the kinematic viscosity. The new laboratory data will determine whether a similar relationship exists after incorporating the refinements introduced above.

Laboratory Experiment

Laboratory experiments on a model radial gate were conducted in 2004 and 2005 at the U.S. Water Conservation Laboratory before it was closed in 2006. Experiments were conducted in two configurations: 1) a downstream channel with the same width as the gate; and 2) a wider downstream channel. A plan view of this experimental setup is shown in Figure 2.

A 1.219-m (4-foot) wide (b_0), 0.610-m (2-foot) high, 15.24 m (50-ft) long glass-sided flume was used to perform the tests. Water was supplied from a constant head tank and discharges were weighed in a large weigh-tank and scale system. The radial gate was 0.457 m wide ($b_1 = b_2$) and had a radius (r), of 0.457 m, with a 3-mm-thick leaf and sharp metal edge gate lip. The gate was set between two 17.5-mm-thick by 1.219-m-long plexiglass side walls. Two quarter-circle pieces of sheet metal were used to narrow the channel by roughly 0.38 m on each side. The layout was modified by adding a 1.22 m long approach section, with the same width as the gate, between the gate chamber and the rounded transition. Surface waves were observed in the approach channel, so a floating surface skimmer was placed immediately downstream from the rounded transition to remove them before the upstream pressure measurement. The trunnion pin height, T, was 0.366 m, located 0.091 m upstream from the downstream end of the side walls, which, if scaled, is typical of installations at the Salt River Project in Phoenix, AZ, from whom the experimental gate was obtained. The gate seat was located 0.854 m downstream from the gate chamber entrance. Downstream water depths were measured 4.6 m downstream from the trunnion pin. Additional details of the hydraulics lab facility can be found in Clemmens et al. (2003).

The upstream and downstream water levels were measured with point gauges in stilling wells outside the glass flume. The pressure was siphoned from 2-cm diameter static tubes set near the floor. Upstream water levels were measured in both the full-width channel (Section 0) and in the gate chamber (Section 1).   The water levels at Section 2 were measured with the static side of a 5 mm-diameter Prandtl tube placed in the middle of the stream. The depth of water at Section 2 under free-flow conditions was also measured with a point gauge. All water levels and pressures were registered to the channel invert elevation immediately under the gate. The floor of the glass sided flume was stainless steel. The floor was set to a level position. The point gauge precision was 0.1 mm.

All depth and flow measurements were collected each time a pressure measurement was taken within the vena contracta. Thus, those measurement conditions were observed multiple times. Slight variations were noted, even though conditions should have been stable. These measurements were generally different by fractions of a millimeter, but some larger deviations were noted. The results for each set of measurement conditions were pooled, and the average value of all measurements was treated as a single "Run." This helped remove some of the random noise in the results.

Tel (2000) used this same facility to conduct a limited number of free-flow tests, at one gate opening. Clemmens et al. (2003) used the data set from Tel (2000). The tests reported here were conducted with a wider range of conditions.

Table 1 shows the conditions that were established for each free-flow run. These were chosen to give a wide range for w/H_1. Each run was repeated several times. Before each test, standing water was used to register point gauges to one another and to the bottom of the channel. Machined blocks of the desired thickness were used to set the gate position, and the gate was clamped in place. The weir at the downstream end of the glass-sided flume was lowered to eliminate tailwater on the gate. The flow was turned on and the supply valve was opened to provide the desired upstream depth under free gate-controlled flow. Flow was stabilized for at least 20 minutes. All depth and pressure measurements were made. Several weight-tank measurements of flow were made while collecting these data.

During initial tests, more extensive measurements of the pressure in the vena contracta were made. One issue was to determine the location of the vena contracta downstream from the gate. Another issue was the pressure distribution within the vena contracta. The depth and pressure at the vena contracta were measured at 3 locations across the width of the channel, roughly at ¼, ½, and ¾ of the width. These pressures were taken at roughly 1 cm below the free surface and 1 cm above the floor, and at roughly 2 cm intervals in between, at the same width locations described above. This was done for several tests.

Calibration

The data collected from the USWCL during 2004 and 2005 were used to determine the pressure distribution coefficients, energy loss coefficients, and contraction coefficients for free flow. The energy equation with these coefficients was used to compute the free-flow discharge for the data collected in 2004 and 2005 (USWCL data), the data collected by Tel (2000) at the same facility, and the data collected by Buyalski (1983) for a sharp-edged gate.

The Buyalski data was collected from a gate and half-pier that were placed in a channel that was slightly wider than the gate, both upstream and downstream. Buyalski measured water levels in the full width channel but reported the downstream water levels as if the channel was the same width as the gate. Wahl (2005) computed the velocity head difference to adjust the downstream depths back to the actual channel width, assuming no head losses were applied in Buyalski's adjustment process. The energy equation relates the head in the full-width upstream channel, H_0, to the conditions in the gate chamber upstream from the gate (section 1)

$$H_0 = \lambda_{E0} y_0 + \alpha_0 \frac{v_0^2}{2g} = \lambda_{E1} y_1 + \alpha_1 \frac{v_1^2}{2g} + \xi_{01}\left(\frac{v_1^2}{2g} - \frac{v_0^2}{2g}\right) \quad (8)$$

where ξ_{01} is the energy-loss coefficient. The Buyalski layout had a more abrupt transition than the USWCL layout. The USWCL layout had a width of 1.231 m contracting to a 0.452 m wide gate and a curved transition with a radius of about 0.38 m. The Buyalski channel was 0.76 m wide and the gate was 0.71 m wide. The transition geometry was not described in detail but appears in his figures to have a radius equal to the width change, or 0.05 m. This smaller radius transition probably functioned more like a blunt transition with ξ_{01} = 0.5. The upstream depths reported by Buyalski were converted to water depth in the gate chamber with Eq. 8 using the measured discharge and ξ_{01} = 0.5.

Tel measured the water depth in the gate chamber (y_1). The depths he reported were the depths in the approach (full-width) channel (y_0), adjusted to account for the difference in velocity head between sections 0 and 1. We used the same procedure to convert back to the original gate chamber depth (y_1). No energy correction needs to be applied to the measured gate chamber depth.

Results

Entrance losses

The entrance contraction energy-loss coefficient was computed for all runs of the USWCL data set where water depths were measured in both Sections 0 and 1. The results are shown in Figure 3. There is considerable scatter in the data. The average value of ξ_{01} was 0.23.

Because standing waves sometimes occurred in the gate chamber, the pressure measured there was not always reliable. There were cases where the depth in the gate chamber was greater than the depth in the upstream channel. The water surface in the upstream channel was always relatively tranquil. Where a depth was measured in the upstream channel, a depth was computed in the gate approach channel from Eq. (8) with ξ_{01} = 0.23. Using this depth did not significantly reduce the scatter in the data and did not resolve any outliers in prediction of discharge. Results from the recalculated depth in the gate approach channel are not reported.

Pressure-Distribution Coefficients (λ_{E2})
Static pressures measured in the laboratory demonstrated that the pressure distributions in the jet downstream from a radial gate are not hydrostatic, with much higher pressures at greater distances below the free surface. This is consistent with the effects of streamline curvature. The observed behavior was essentially the same at all horizontal locations. Pressure distribution coefficients were obtained by numerically integrating the observed pressures. Figure 4 shows values of λ_{E2} from the experimental data. For many data sets, only two pressures were taken: one near the surface and one near the bottom. These gave only approximate values of λ_{E2}, based on three line segments: hydrostatic pressure at the surface to upper pressure reading, upper to lower pressure readings, and lower pressure reading extended as a constant value to the floor. These are labeled as "USWCL Free 2 pt."

The equation fit to the data is:

$$\lambda_{E2} = 1.06 - 0.21\,\frac{y_2}{H_1} + 0.15\left(\frac{y_2}{H_1}\right)^2 \qquad (9)$$

Examples of the measured pressure distributions are shown in Figure 5, for different values of y_2/H_1. This graph shows the measured static pressure relative to the measured water depth. If the pressures are hydrostatic, the relative pressure would be 1. Note that at low values of relative depth (y_2/H_1) where free flow exists, the pressures are above hydrostatic at all vertical locations. As y_2/H_1 increases, the pressures start to drop below hydrostatic just below the water surface. The relative depth is 0 at the floor and 1 at the water surface.

No measurements were taken for the pressure distribution upstream from the gate, so hydrostatic pressure is assumed, with λ_{E1} = 1.0.

Gate Contraction Coefficient, δ
Based on the USWCL data, a best fit relationship was found for the gate contraction coefficient $\delta(\theta,a)_F$ as a function of the gate lip angle θ and $a = w/H_1$. These coefficient values were found manually to minimize the sum of squares of deviations between measured and predicted gate openings. The resulting relationship is:

$$\delta\left({}^{\pi}/_{2}, 0\right)_F = 0.682 \qquad (10a)$$

$$\delta(\theta,0)_F = 1 - 0.3179\theta + 0.007\theta^2 + 0.0494\theta^3 - 0.0045\theta^4 \qquad (10b)$$

$$\delta(\theta,a)_F = \delta(\theta,0)_F + [1 - \delta(\theta,0)_F]\{-0.397a - 0.035a^2 + 0.34a^3 + 0.675a^4\} \qquad (10c)$$

Eq. (10) gives a value of 1.0 for the gate contraction coefficient at $\theta = 0$; i.e., like a perfectly streamlined nozzle. The results for δ_F as a function of θ are shown in Figure 6. The best fit line is from Eq. (10b). This equation is an extrapolation to $a = 0$. It does not fit the data directly since there are no measured values at $a = 0$. Note that the value of δ_F at $\pi/2$ (0.682) is higher than the value of 0.611 suggested by Montes (1997) for ideal flow and slightly higher than the value of 0.649 determined by Belaud et al. (2009) for a value of $\alpha_2 = 1.04$. Tel (2000) did not consider the effect of w/H_1, so the fit is quite different.

Figure 7 shows the value of δ_F as a function of $a = w/H_1$ from Eq. (10c), for $\theta = \pi/2$ (roughly 1.57). The fitted curve lies slightly above the Belaud et al. (2009) curve for $\alpha_2 = 1.04$. The Belaud curve for $\alpha_2 = 1.00$ is even lower. The data used to develop the relationship was collected for the range of θ from roughly 0.8 to 1.2, but the curve represents an extrapolation of the measured data to $\theta = \pi/2$ (roughly 1.57). Thus, the deviation from the Belaud et al. (2009) relationship is not surprising. The data for each value of gate opening, and thus θ, are shown in Figure 7 along with the predicted relationship (Line). The error in predicted δ_F for Eq. (10) is shown in Figure 8. One data point was found to be an outlier (more than 5 standard deviations from mean).

Gate Energy Loss Coefficient, ξ_2

Eq. (4) can be rearranged to solve for ξ_2.The value of ξ_2 can be determined from Eq. (4) with measured values of b_2, Q and y_j (δw), a known value for $g = 9.807$ m/s^2, an assumed value of $\alpha_2 = 1.04$, and λ_{2E} from Eq. (9). Two different methods were explored for determining the energy loss for flow through the gate, ΔH_{12}. These include:

$$\Delta H_{12} = \xi_2 \left(\frac{v_2^2}{2g}\right) \quad (11a)$$

$$\Delta H_{12} = \xi_{12} \left(\frac{v_2^2}{2g} - \frac{v_1^2}{2g}\right) \quad (11b)$$

The first method is that used by Clemmens et al. (2003) and used to develop Eq. (4). The second method is attempting to determine loss as a function of change in velocity head. This approach did not prove to be more useful than the first method and the energy equation is slightly more complicated. Based on this analysis, the energy loss is predicted based only on the vena contracta velocity, as in Clemmens et al. (2003).

The data from Buyalski (1983) did not include measurement of the vena contracta depth. Thus, the energy loss cannot be estimated from measured data. To overcome this, the contraction coefficient from the observed USWCL data was used. Using this method for all three data sets provided more refined estimates of the loss coefficient, as shown in Figure 9. This analysis showed that $\delta_F(w/H_1)$ or y_{2F}/H_1 provided a better estimate of ξ_2 than Reynolds number. The resulting relationship is

$$\xi_2 = K_\xi \, \delta_F w/H_1 \quad (12)$$

The value of K_ξ is 0.195 for the raw USWCL data. Using Eq. 10 to define the contraction coefficient gave values of K_ξ of 0.199 for the USWCL data and 0.210 for all three data sets combined. Figure 9A shows the results from the raw data while Figure 9B shows the results when δ is determined from Eq. 10 for all three data sets. The slope of the line is K_ξ. There were two outliers (more than 3 standard deviations from regression estimate) in the USWCL data.

Free-Flow Discharge Prediction

Once values for δ, λ_{E1}, λ_{E2}, α_1, α_2 and ξ_2 are known, the discharge under free flow can be computed from Eq. (4) with measured values of b_2, y_1 and w. The value of θ is found from gate opening, w, and gate geometry. The value of δ is found from Eq. (10). The following values were used for the other parameters; $\lambda_{E1} = 1$, $\alpha_1 = 1.04$, $\alpha_2 = 1.04$, λ_{E2} is computed from Eq. (9), and ξ_2 is computed from Eq. (12). Solution of Eqs. (4), (9), (10) and (12) is iterative since the velocities are dependent on the discharge. Iterations start with any discharge, even Q=0. Then the velocity v_1 is calculated followed by the energy head H_1 and the rest of the terms from Eqs. (9), (10) and (12), Solving Eq. (4) gives a discharge and the process is repeated until the discharge converges. These equations were solved for free-flow runs from the USWCL laboratory data, Tel (2000) data and Buyalski (1983) data. The results are shown in Figure 10 and Table 2. The accuracy values are (predicted-measured)/(free-flow) value. Table 2 shows simple numerical averages and standard deviations.

Figure 10A shows the results when ξ_2 is found from the USWCL raw data, with $K_\xi = 0.195$. Table 2, column 2 shows the numerical results. As expected, the USWCL errors are minimized. Figure 10B shows the results when ξ_2 is found from all data sets, with δ from Eq. (10), which is required for the Buyalski data since contraction coefficients were not measured. Table 2, column 4 shows the numerical results. A value of $\xi_2 = 0.210$ gives the minimum value of the mean square error in discharge. With both methods, the Buyalski errors are almost 1% higher than the USWCL errors.

Discussion

The range of $a = w/H_1$ observed in this data set was 0.110 to 0.713. Attempts to obtain higher values of a were unsuccessful. At the lower upstream water depths associated with higher values of a, flow passed under the gate. No attempt was made to define the conditions under which this occurred.

The location of the vena contracta was measured during several of the early runs by locating the point of minimum depth. The commonly used value is 2 times the gate opening downstream from the gate lip. In some cases, measurements showed it to be as much as 3 or 4 times the gate opening downstream. It is possible that the location of the vena contracta is a function of gate angle and/or w/H_1, but this was not examined in detail. Further evaluation of this length should be investigated in future research.

The results for free flow are sufficiently accurate to meet typical flow-measurement objectives. The empirical, best-fit results for the contraction coefficient gave better results than use of relationships from Belaud et al. (2009). Further improvements in these equations might be possible. Submerged flow has proven to be more challenging. The results for submerged flow will be presented in a future paper using a method starting from the free-flow approach presented here.

Earlier versions of this method (Clemmens et al., 2003 and Wahl, 2005) have been programmed into a software package for determining check structure discharges (with multiple gates) to make these result easier to use in practice. This software package is described in Wahl and Clemmens (2012). The software will be updated with these new relationships.

Conclusions

Pressure-distribution, velocity-distribution, energy loss, and contraction coefficients were developed for free flow radial gates. The pressure distribution coefficient was a function of the ratio of vena contracta depth to upstream energy head, y_2/H_1. The contraction coefficient was a function of both gate lip angle, θ, and relative gate opening $a = w/H_1$. The energy loss through the gate chamber to the vena contracta was effectively modeled as a function of vena contracta velocity. A relationship was developed for the gate loss coefficient as a function of relative gate opening.

Laboratory data from three sources were used to compare observed flow rates to solution of the energy equation, with the coefficients derived from the USWCL laboratory data. The prediction accuracy (95% confidence interval) with these results was within roughly ± 2%. Submerged flow will be examined in a future paper.

Data Availability Statement

The raw data in an Excel spreadsheet are available from the corresponding author upon reasonable request. Raw data as input to WinGate is also available.

Acknowledgement

This research was supported by the USDA Agricultural Research Service and the US Bureau of Reclamation.

References

Belaud, G., Cassan, L., and Baume, J-P. 2009. Calculation of contraction coefficient under sluice gates and application to discharge measurement. *Journal of Hydraulic Engineering*, 135(12):1086-1091. https://doi.org/10.1061/(ASCE)HY.1943-7900.0000122

Belaud, G., Cassan, L. and Baume, J.-P. 2012 Contraction and correction coefficients for Energy-Momentum balance under sluice gates. Proceedings of the 2012 World Environmental & Water Resources Congress, Albuquerque, NM, May 20-24, 2012, ASCE, Reston, VA, 2116-2127. https://doi.org/10.1061/9780784412312.212

Buyalski, C.P. 1983. Discharge Algorithms for Canal Radial Gates. U.S. Department of the Interior, Bureau of Reclamation, Research Report REC-ERC-83-9, Denver, CO.

Cassan, L. and Belaud, G. 2012. Experimental and numerical investigation of flow under sluice gates. *Journal of Hydraulic Engineering*, 138(4):367-373. https://doi.org/10.1061/(ASCE)HY.1943-7900.0000514

Clemmens, A.J. and Wahl, T.L. 2012. Computational procedures used for radial gate calibration in WinGate. Proceedings of the 2012 World Environmental & Water Resources Congress, Albuquerque, NM, May 20-24, 2012, ASCE, Reston, VA, 2106-2115. https://doi.org/10.1061/9780784412312.211

Clemmens, A.J., Wahl, T.L., Bos, M.G., and Replogle, J.A. 2001. Water Measurement with Flumes and Weirs. Publication No. 58, International Institute for Land Reclamation and Improvement, Wageningen, The Netherlands. 382 pp.

Clemmens, A.J., Strelkoff, T.S., and Replogle, J.A. 2003. Calibration of submerged radial gates. Journal of Hydraulic Engineering, 129(9):680-687. https://doi.org/10.1061/(ASCE)0733-9429(2003)129:9(680)

Henderson, F.M. 1966. Open Channel Flow. MacMillan Publishing Co., Inc., New York.

Montes, J.S. 1997. Irrotational flow and real fluid effects under planar sluice gates. *Journal of Hydraulic Engineering*, 123(3):219-232. https://doi.org/10.1061/(ASCE)0733-9429(1997)123:3(219)

Tel, J. 2000. Discharge Relations for Radial Gates. MSc Thesis, Delft Technical University, Delft, The Netherlands, 86 pp. plus Appendices.

Wahl, T.L. 2005. Refined energy correction for calibration of submerged radial gates. *Journal of Hydraulic Engineering*, 131(6):457-466. https://doi.org/10.1061/(ASCE)0733-9429(2005)131:6(457)

Wahl, T.L. and Clemmens, A.J. 2012. WinGate software for discharge calibration of gated check structures. Proceedings of the 2012 World Environmental & Water Resources Congress, Albuquerque, NM, May 20-24, 2012, ASCE, Reston, VA, 2206-2212.

Notation

a – w/H_1
b – bottom width
g – acceleration of gravity
H – energy head
K – empirical constant
Q – discharge
r – gate radius
Rh – hydraulic radius
Re – Reynolds Number
T – trunnion-pin height
v – velocity
w – gate opening

y – water depth
α – velocity distribution coefficient
Δ - change
δ – contraction coefficient
ξ – energy loss coefficient
λ – pressure distribution coefficient
π – ratio of circumference to diameter of circle
θ – gate lip angle
Subscripts
0 – upstream section
1 – gate chamber upstream from gate
2 – location of the gate vena contracta
3 - measurement location downstream from gate
E – associated with energy equation
F – free-flow conditions
ξ - associated with energy loss

List of Figures

Table 1. Experimental free-flow test conditions.

Upstream head y_1 (m)	Gate Opening w (m)	Expected y_2 for free flow (m)
0.45	0.05	0.0375
0.48	0.10	0.0709
0.48	0.15	0.1013
0.40	0.05	0.0375
0.40	0.20	0.1299
0.33	0.05	0.0375
0.33	0.10	0.0709
0.33	0.20	0.1299
0.30	0.15	0.1013
0.30	0.20	0.1299
0.25	0.05	0.0375
0.15	0.10	0.0709
0.13	0.05	0.0375

Table 2. Free-flow discharge accuracy

	When ξ_2 fit to USWCL Data with measured δ	When ξ_2 fit to USWCL data with C_c from Eq. 10	When ξ_2 fit to All data with C_c from Eq. 10
	$K_\xi = 0.195$	$K_\xi = 0.199$	$K_\xi = 0.210$
Overall			
Average Error	0.37%	0.32%	0.20%
Standard Deviation	0.96%	0.97%	0.99%
Mean Square Error	1.03%	1.02%	1.01%
USWCL			
Average Error	-0.04%	-0.09%	-0.25%
Standard Deviation	0.88%	0.87%	0.85%
Mean Square Error	0.88%	0.87%	0.88%
Tel			
Average Error	0.07%	0.01%	-0.15%
Standard Deviation	1.19%	1.19%	1.20%
Mean Square Error	1.19%	1.19%	1.21%
Buyalski			
Average Error	0.68%	0.64%	0.54%
Standard Deviation	0.85%	0.86%	0.90%
Mean Square Error	1.25%	1.24%	1.22%

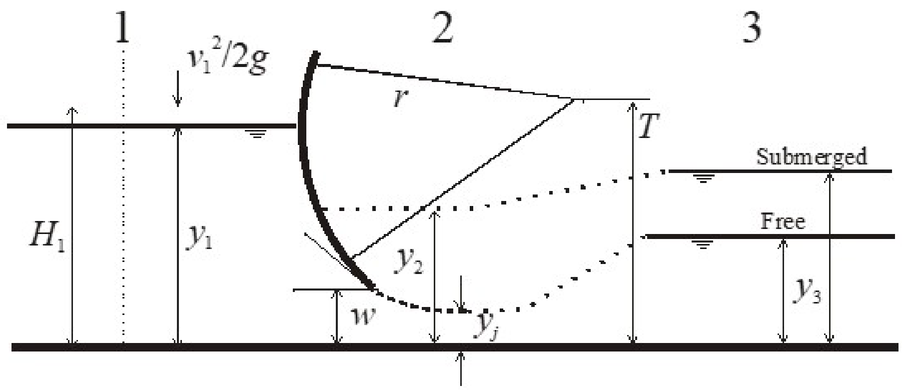
1
2
3
$v_1^2/2g$
r
T
Submerged
Free
H_1
y_1
y_2
y_3
w
y_j

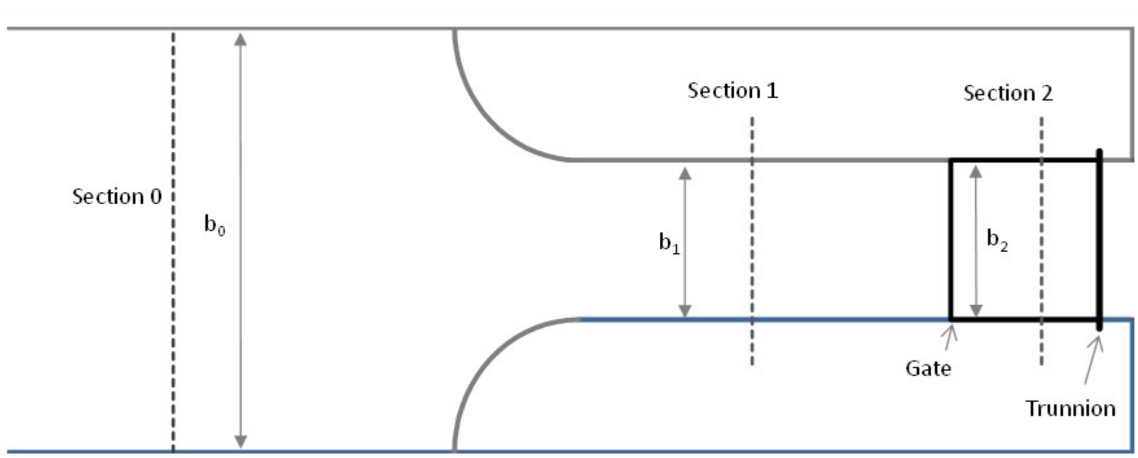
Section 0
b_0
Section 1
b_1
Section 2
b_2
Gate
Trunnion

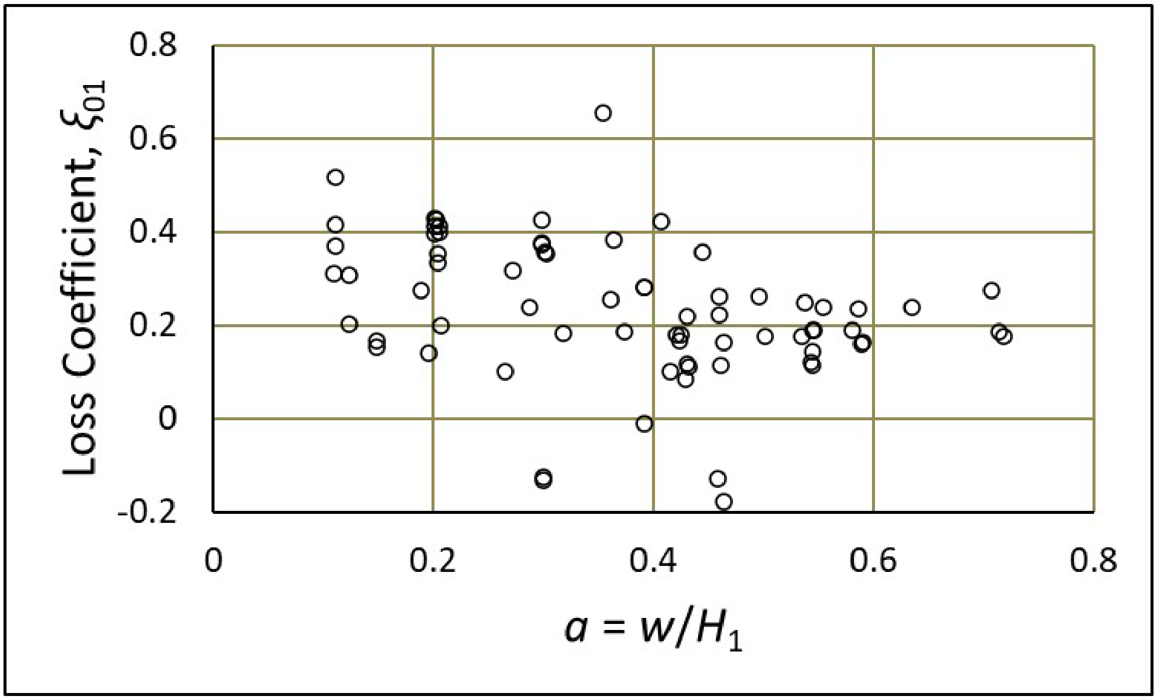
0.8
0.6
0.4
0.2
0
-0.2
Loss Coefficient, ξ_{01}
0
0.2
0.4
0.6
0.8
$a = w/H_1$

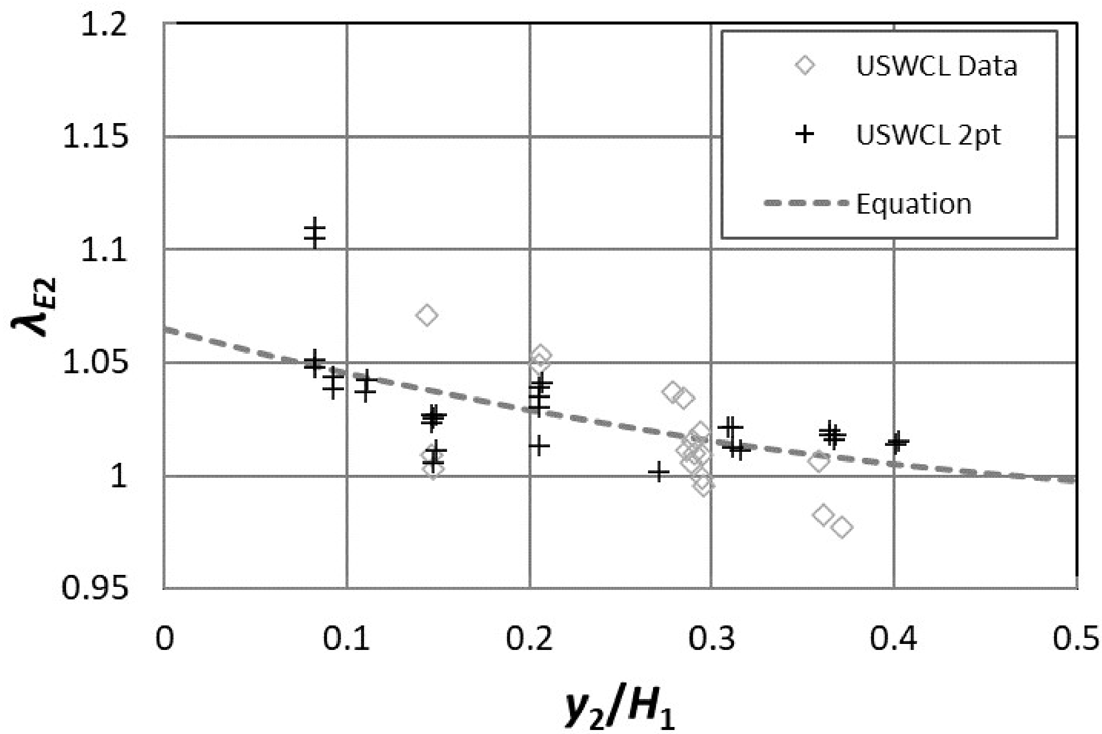
USWCL Data
USWCL 2pt
Equation
λ_{E2}
y_2/H_1
1.2
1.15
1.1
1.05
1
0.95
0
0.1
0.2
0.3
0.4
0.5

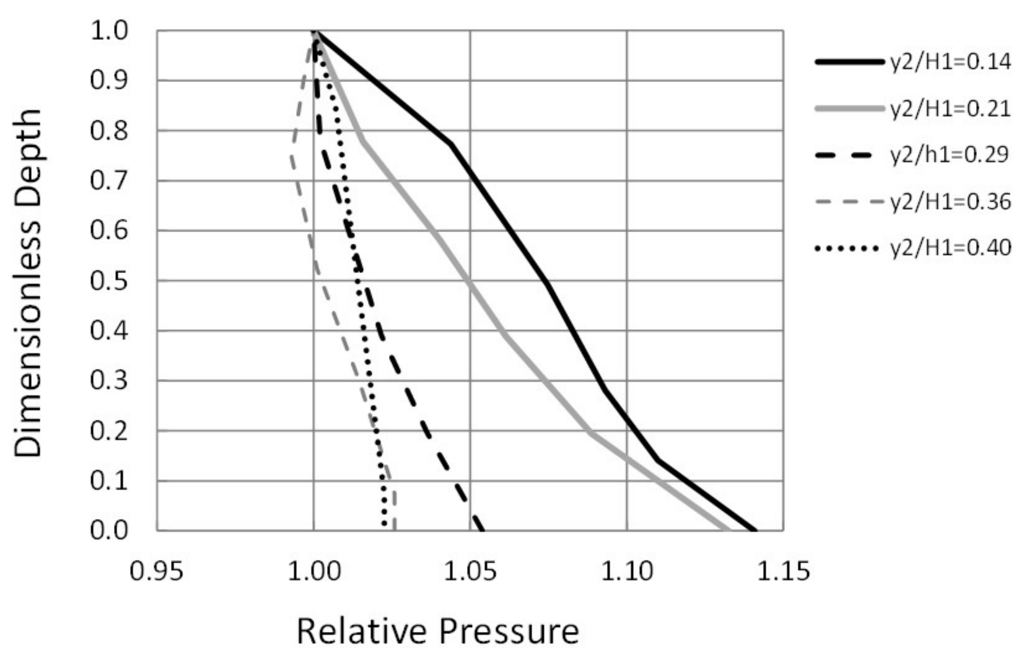
y2/H1=0.14
y2/H1=0.21
y2/h1=0.29
y2/H1=0.36
y2/H1=0.40
Dimensionless Depth
Relative Pressure
1.0
0.9
0.8
0.7
0.6
0.5
0.4
0.3
0.2
0.1
0.0
0.95
1.00
1.05
1.10
1.15

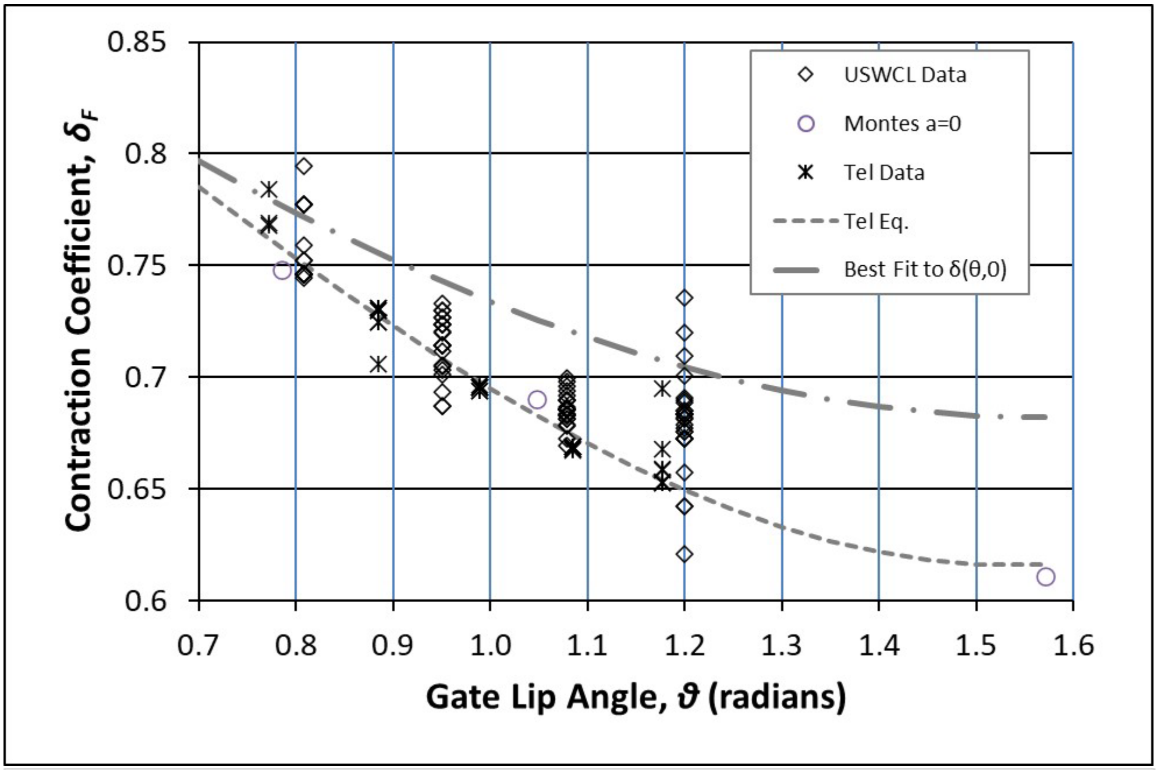

Contraction Coefficient, δ_F
Gate Lip Angle, ϑ (radians)
USWCL Data
Montes a=0
Tel Data
Tel Eq.
Best Fit to δ(θ,0)

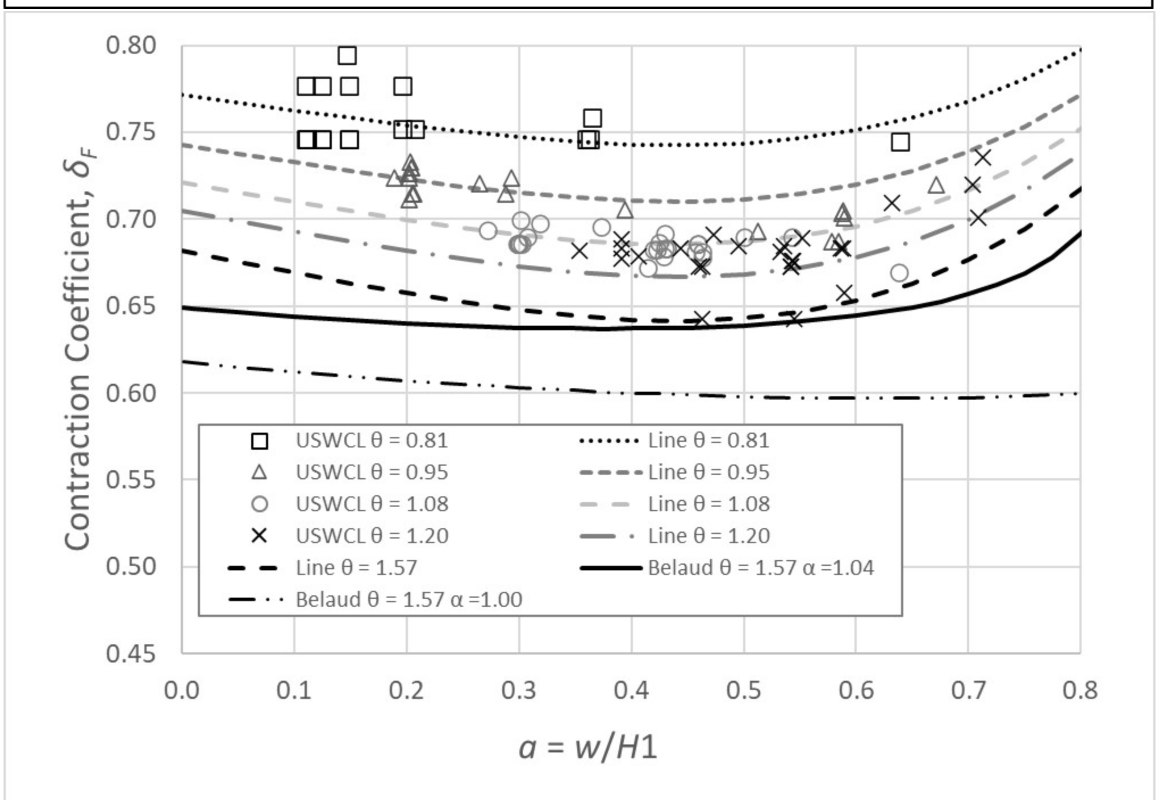

Contraction Coefficient, δ_F
$a = w/H1$
USWCL θ = 0.81
USWCL θ = 0.95
USWCL θ = 1.08
USWCL θ = 1.20
Line θ = 1.57
Belaud θ = 1.57 α =1.00
Line θ = 0.81
Line θ = 0.95
Line θ = 1.08
Line θ = 1.20
Belaud θ = 1.57 α =1.04

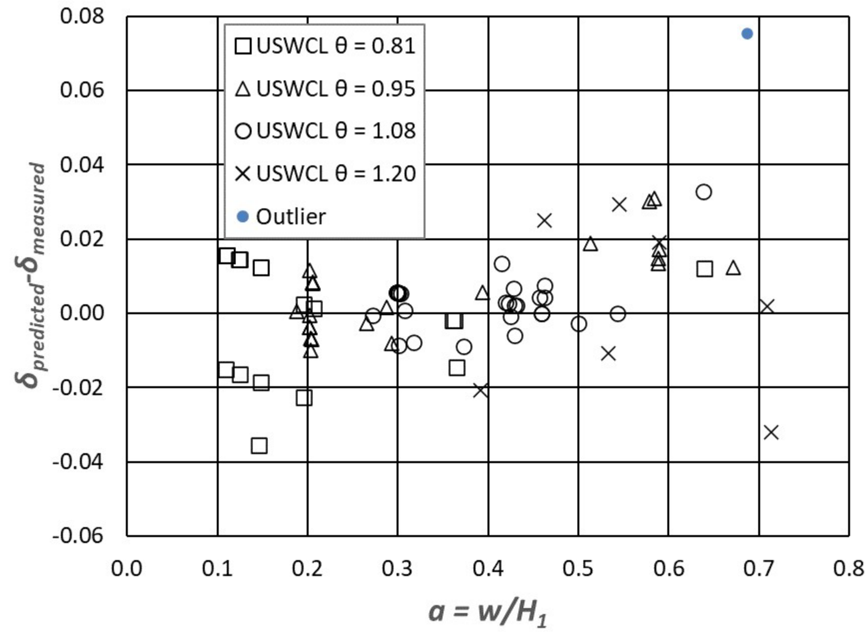
USWCL θ = 0.81
USWCL θ = 0.95
USWCL θ = 1.08
USWCL θ = 1.20
Outlier
0.08
0.06
0.04
0.02
0.00
-0.02
-0.04
-0.06
0.0
0.1
0.2
0.3
0.4
0.5
0.6
0.7
0.8
δpredicted-δmeasured
a = w/H1

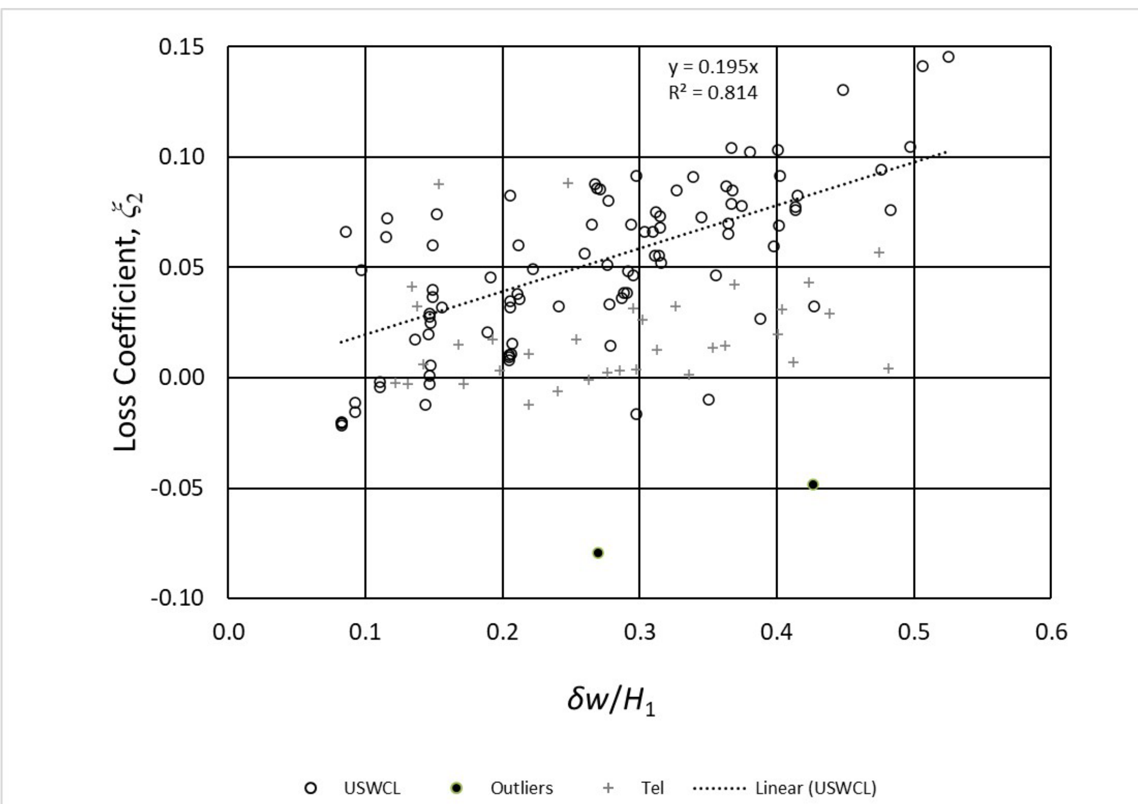
y = 0.195x
R² = 0.814
0.15
0.10
0.05
0.00
-0.05
-0.10
0.0
0.1
0.2
0.3
0.4
0.5
0.6
Loss Coefficient, ξ2
δw/H1
USWCL
Outliers
Tel
Linear (USWCL)

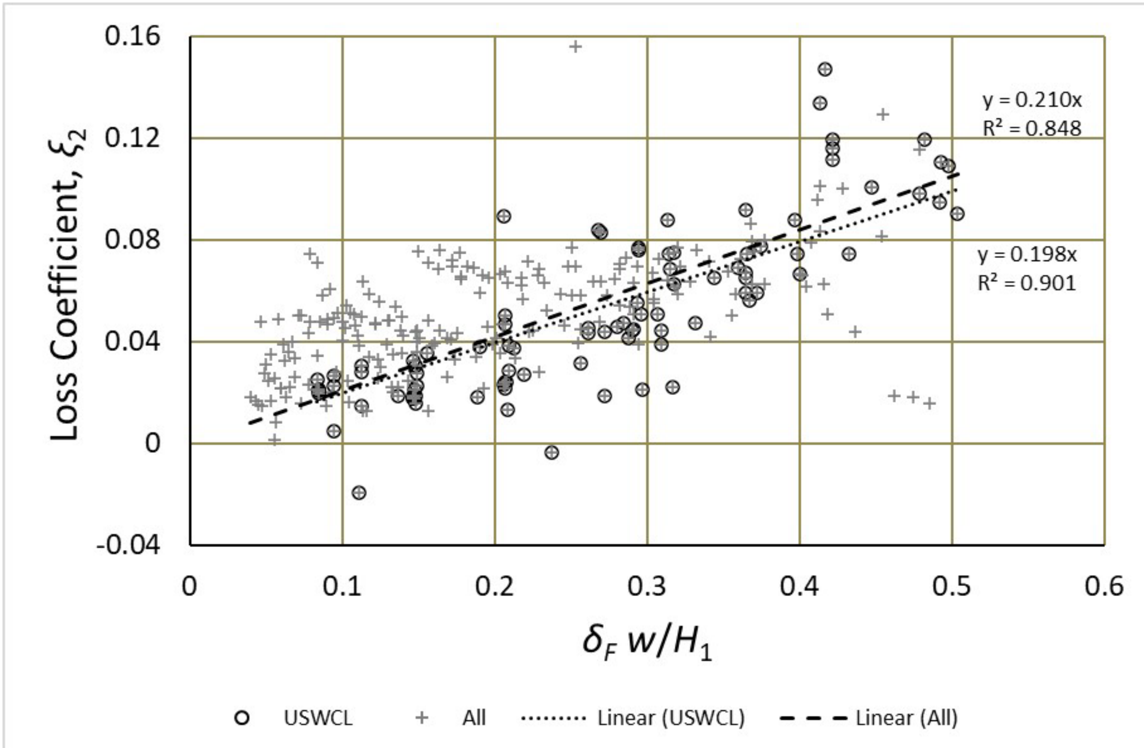

Loss Coefficient, ξ_2
$\delta_F\ w/H_1$
y = 0.210x
R² = 0.848
y = 0.198x
R² = 0.901
USWCL
All
Linear (USWCL)
Linear (All)

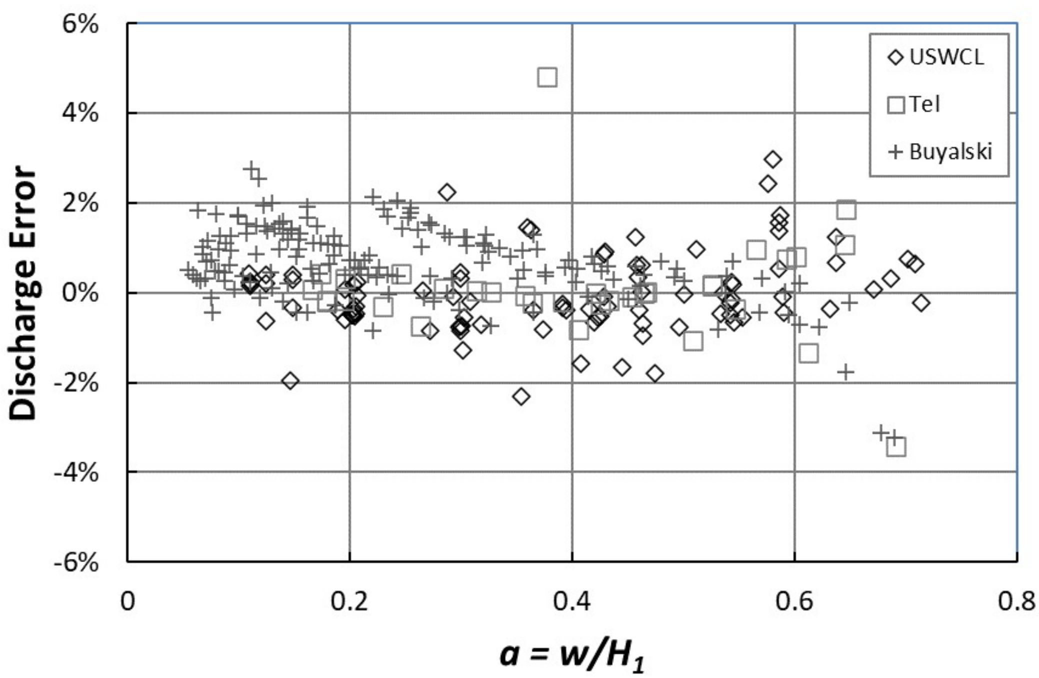

Discharge Error
$a = w/H_1$
USWCL
Tel
Buyalski

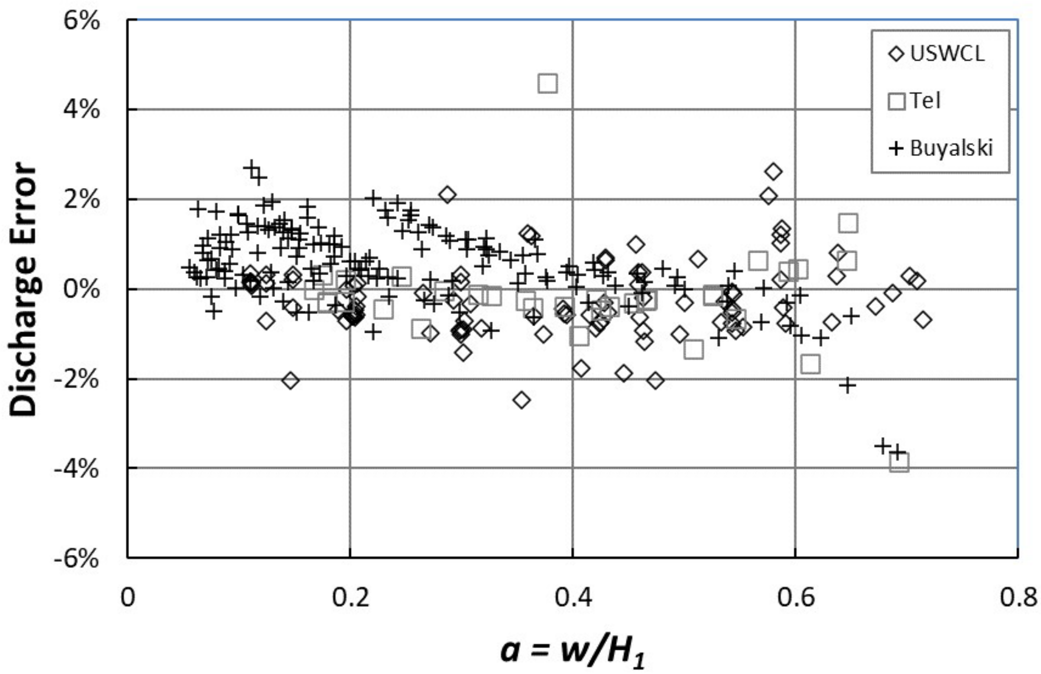
6%
4%
2%
0%
-2%
-4%
-6%
Discharge Error
0
0.2
0.4
0.6
0.8
a = w/H1
USWCL
Tel
Buyalski